



First results from the Juice magnetometer during the Lunar-Earth Gravity Assist

Adrian T. LaMoury¹, Leonard Schulz², Alexander Betzler^{3,4}, David Hercik⁵, Hans-Ulrich Auster², Patrick Brown¹, Werner Magnes³, Christoph Amtmann³, Richard Baughen¹, Hao Cao⁶, Irmgard Jernej³, Roland Lammegger⁴, Adam Masters¹, Ferdinand Plaschke², Xun Yu¹, Taylor Pomfret¹, Alex Strickland¹, Vaibhav Garg¹, and Michele K. Dougherty¹

¹Blackett Laboratory, Imperial College London, London, UK

²Institut für Geophysik und extraterrestrische Physik, Technische Universität Braunschweig, Braunschweig, Germany

³Space Research Institute, Austrian Academy of Sciences, Graz, Austria

⁴Institute of Experimental Physics, Graz University of Technology, Graz, Austria

⁵Institute of Atmospheric Physics, Czech Academy of Sciences, Prague, Czechia

⁶Department of Earth, Planetary, and Space Sciences, University of California, Los Angeles, Los Angeles, USA

Correspondence: Adrian T. LaMoury (adrian.lamoury15@imperial.ac.uk)

Abstract. Before reaching the Jovian system in 2031, the ESA Jupiter Icy Moons Explorer (Juice) spacecraft will perform three Earth flybys. As well as providing gravitational assistance, these flybys are prime opportunities to assess performance and undertake in-flight calibration of the science payload in a well-understood environment. The first such interval occurred in August 2024, dubbed the Lunar-Earth gravity assist (LEGA) as it included a pass by the Moon in advance of the approach to Earth. The unique spacecraft trajectory allowed for sampling of various regions of the magnetosphere before exiting into the solar wind. In this paper, we report on the performance of the Juice magnetometer instrument (J-MAG) during the LEGA. J-MAG comprises three sensors—two fluxgate vector sensors and one Coupled Dark State Magnetometer (CDSM) scalar sensor—all of which were operational during the LEGA period. This represents the first time in the mission that the scalar sensor has operated in its nominal state. Here, we analyse J-MAG observations during key periods of the flyby. As well as inter-sensor comparison, we assess J-MAG data against geomagnetic field models during the approach to Earth, and compare with measurements from other spacecraft at the Moon and in the solar wind, which allow us to make suggestions for future calibration activities. Overall, the three sensors showed excellent performance at this early stage in the mission and confirmed that the scalar sensor meets the requirements for in-flight calibration of the fluxgate sensors at Ganymede. The LEGA also demonstrates the potential value of using cruise phase measurements for scientific exploration and solar wind monitoring.

1 Introduction

The European Space Agency's Jupiter Icy Moons Explorer (Juice; see Grasset et al., 2013) launched in April 2023. As part of the mission cruise phase, the spacecraft performs three gravity assists at Earth, the first of which occurred in August 2024, and included a flyby of the Moon. The Lunar-Earth Gravity Assist (LEGA) was an excellent opportunity to gain an early indication of spacecraft and instrument performance in a known environment, allowing for preliminary calibration activities



20 and some exploratory science. In particular, the conditions and phenomena seen in some regions of Earth's magnetosphere, and the performance of J-MAG within them, are indicative of those expected at Ganymede.

In this paper we report on the operation and results from the Juice magnetometer instrument, J-MAG, during the LEGA. There are three sensors that comprise the J-MAG system: the outboard sensor (henceforth referred to as OBS), the inboard sensor (IBS), and the scalar sensor (SCA). All three are mounted on a 10.6 m boom, away from the body of the spacecraft. 25 OBS and IBS are fluxgate magnetometers that draw heritage from those flown on missions such as Cassini (Dougherty et al., 2004), Solar Orbiter (Horbury et al., 2020), Rosetta (Auster et al., 2007), and Bepi Colombo (Heyner et al., 2021). SCA is a Coupled Dark State Magnetometer (CDSM), an optical sensor that uses the Zeeman effect to measure an absolute magnetic field (for background on the scalar sensor engineering and operation see, e.g., Pollinger et al., 2018; Amtmann et al., 2024). Juice is the first mission to use such a magnetometer outside of Earth orbit, and with that comes many additional challenges.

30 This paper focuses on demonstrating the overall performance of the J-MAG system during the LEGA, without detailed discussion of calibration procedures. This is the subject of future study and can only be completed with additional data beyond this early stage of the mission. The report is structured as follows: first we describe the LEGA trajectory and solar wind context in which it occurred. We then describe the timeline of J-MAG operation, with a particular focus on the unique challenges faced by SCA. Then we report on the J-MAG measurements, making comparisons to those from other spacecraft and models where 35 appropriate. This is broken down by particular regions of interest including the close approach to Earth, the lunar pass, the exit from the magnetosphere, and the journey into the solar wind. We conclude with a summary and outlook for future J-MAG operation and calibration opportunities.

2 LEGA trajectory, timeline, and environment

The spacecraft trajectory relative to Earth is shown by the black dashed line in Figure 1. This depicts the X-Y plane in the 40 Geocentric Solar Ecliptic (GSE) coordinate system, with markers showing the spacecraft position at midnight of each day. The portions of the trajectory for which J-MAG was recording science data are highlighted in red. An approximate magnetopause is shown by the solid black line, derived from the Shue et al. (1998) empirical model parametrised using average solar wind conditions over the flyby (see Figure 2).

Juice approached from the nightside, first encountering the Moon on 19th August 2024. For a period of around 40 minutes, 45 the spacecraft was eclipsed by the Moon, and therefore running on battery power, limiting operations. Shortly after eclipse, Juice made its closest approach to the Moon at 21:15, at which the minimum distance from the spacecraft to the centre of the Moon was ~ 2500 km, or approximately 1.5 lunar radii. At this point, the spacecraft was deep in the magnetotail, close to the Sun-Earth line. J-MAG made observations for a two-hour period across the lunar pass. In Sect 3.2, we look at this phase of the flyby in more detail.

50 Following the lunar encounter, Juice continued its approach towards Earth, largely following the Sun-Earth line but veering to the dawn side. The trajectory took the spacecraft round the dayside, headed duskward. Closest approach was made on 20th

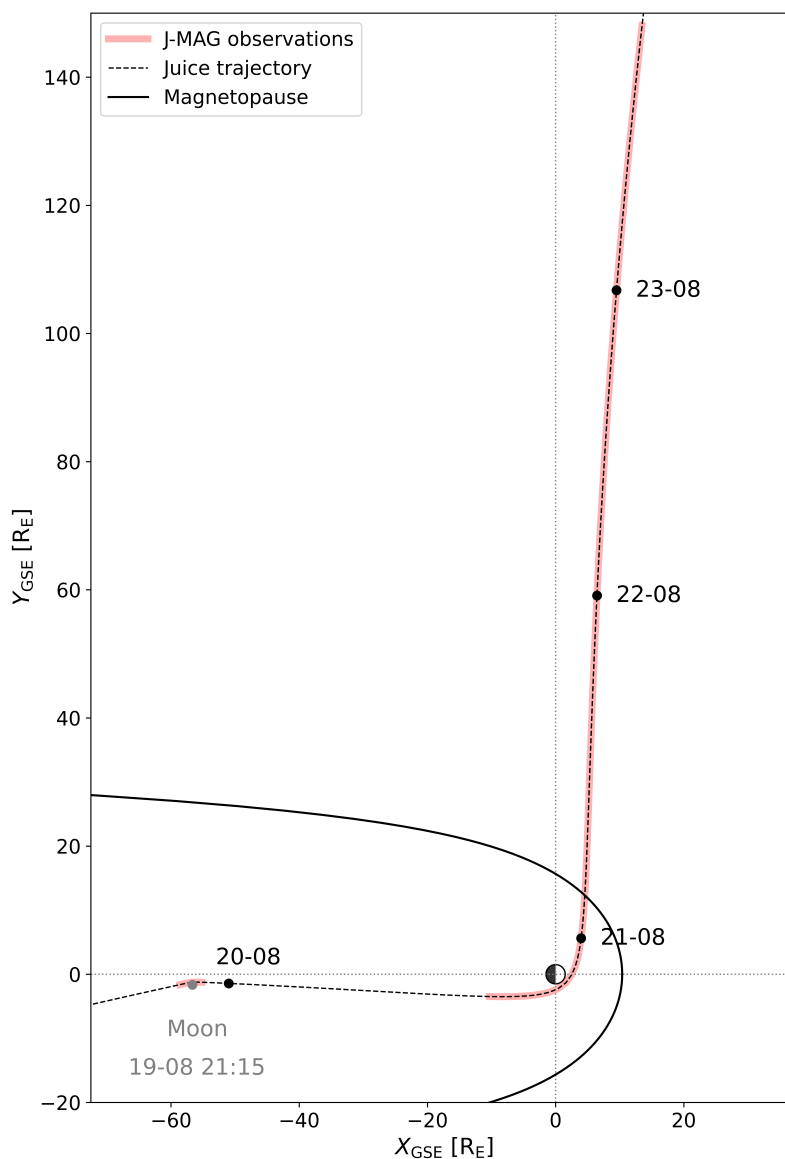


Figure 1. Orbital trajectory of Juice spacecraft during the LEGA, shown in the GSE X-Y plane, in units of Earth radii. Dashed black line shows spacecraft path, with the position at midnight of each day marked with a black dot. The portions of the flyby for which J-MAG was recording science data are highlighted in red. Solid black line shows an approximate position of the magnetopause as predicted by the Shue et al. (1998) empirical model, parametrised with average solar wind conditions during the LEGA period. The position of the Moon at lunar closest approach is also marked.



August at 21:56, at which the distance to the centre of Earth was around $2 R_E$, or $\sim 13,000$ km, taking the spacecraft deep into the inner magnetosphere. J-MAG started recording science data around 4 hours before closest approach.

Juice exited the magnetosphere at around 03:00 on 21st August, crossing the magnetopause, transiting the magnetosheath, and passing through the bow shock around $5 R_E$ sunward of the terminator (see Sect 3.3 for more detail). Thereafter, Juice continued duskward and marginally sunward into the pristine solar wind, with J-MAG operating continuously before switching off on 23rd August.

Figure 2 shows the solar wind context and a more detailed timeline of J-MAG operation during the LEGA. Panel a) shows the solar wind magnetic field as taken from the OMNI database (King and Papitashvili, 2005). The high-resolution (1-min cadence) dataset comprises solar wind measurements made by spacecraft at the L1 Lagrange point (e.g., ACE, Wind, or DSCOVR) and algorithmically propagated to Earth's bow shock, making it the standard and most complete dataset for the solar wind conditions driving Earth's magnetosphere. The second panel shows the solar wind dynamic pressure, also provided by OMNI. This quantity compounds solar wind mass density with its speed, that is, $P_d = \rho V^2$. Dynamic pressure is a key metric for assessing the energy input to the magnetosphere, with higher dynamic pressures typically compressing the magnetosphere and stimulating geomagnetic activity. Panel c) shows a timeline of operation of the three J-MAG sensors, OBS, IBS, and SCA. Also marked on this panel with vertical lines are the moments of closest approach to the Moon and to Earth. Panel d) shows the distance of the spacecraft from Earth throughout the flyby.

Breaking the J-MAG timeline down by sensor, OBS and IBS sensors were switched on at 20:19, just shy of an hour ahead of the lunar closest approach (21:15). Both fluxgates remained on until 22:14 and made observations at 16 Hz cadence. SCA was not operational during the lunar phase (see Sect 2.1). Ahead of the Earth flyby on 20th August, OBS and IBS took measurements from 18:01, with SCA starting shortly after at 18:34. All three sensors then remained on for several days, switching off when the spacecraft was well into the solar wind on 23rd August, SCA at 21:22, OBS and IBS at 21:53. At this point, Juice was $150 R_E$ from Earth.

We see that, during the early portion of the flyby, the solar wind exhibited relatively quiet and stable conditions with low dynamic pressure (solar wind speed was slow, at around 300 km s^{-1}), low magnetic field magnitude and few large variations. There were, however, periods of negative B_z which may have driven reconnection at the magnetopause and short periods of activity. Later on, after Juice left the magnetosphere, activity in the solar wind increased, with a ramp up in both magnetic field magnitude and dynamic pressure. There is also a notable period of rotation in the magnetic field at the point of highest dynamic pressure. This provided an excellent opportunity to compare the structure observed by J-MAG with that seen by spacecraft at L1 (see Sect 3.3).

2.1 Scalar sensor operation

The operation of the scalar sensor is considerably more complicated than the two fluxgate sensors. In this section we detail the process used during the LEGA. The three Juice Earth gravity assists (EGAs) present crucial opportunities for SCA as they are the only times during the cruise phase when SCA can make a direct measurement of the external field magnitude. By this we mean that the CDSM is not suitable for measurements below 100 nT with high accuracy (Ellmeier et al., 2024) and so in

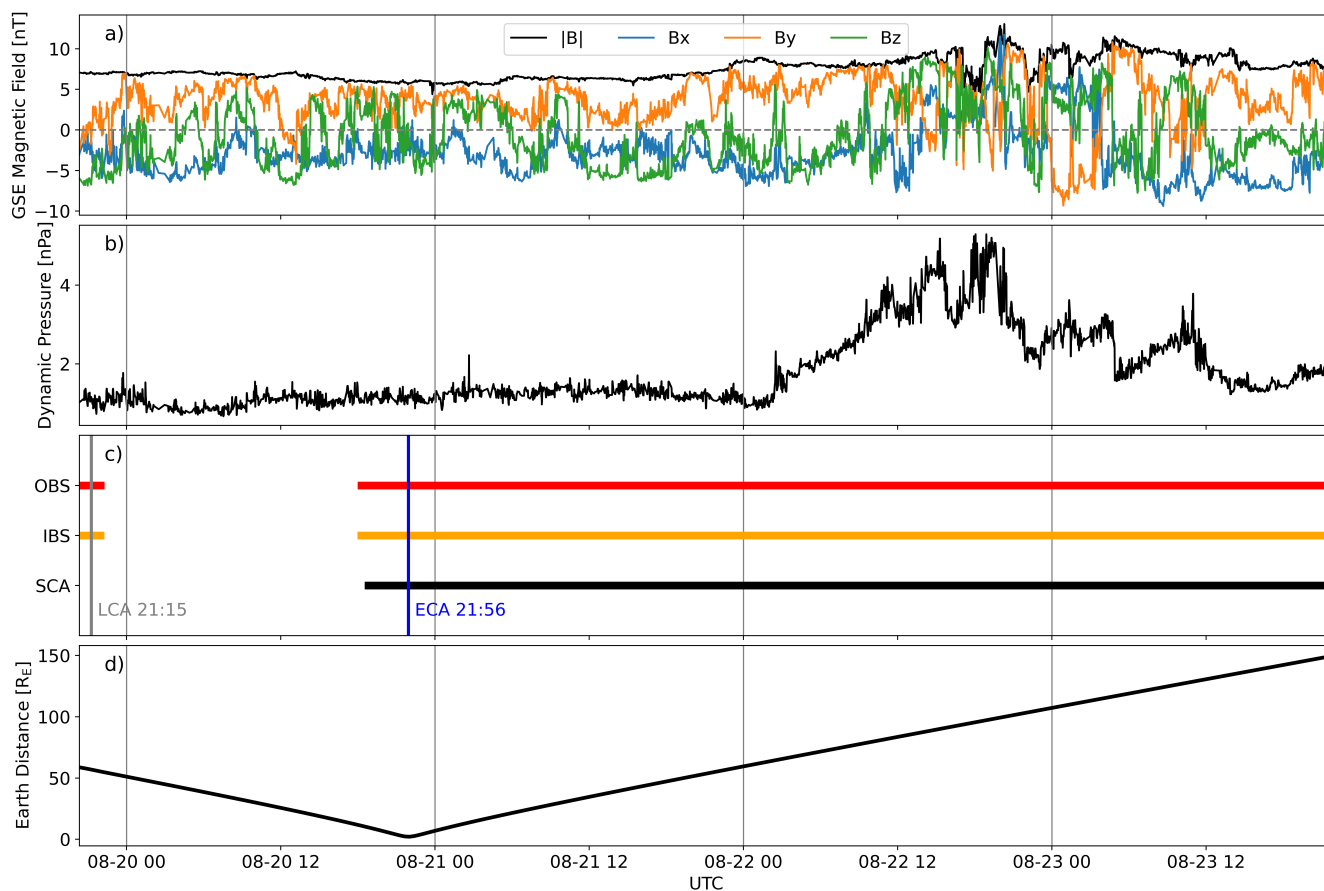


Figure 2. Flyby context and timeline. Panel a) shows the solar wind magnetic field (GSE) from the OMNI database, that is, measured at L1 and algorithmically propagated to Earth’s bow shock. Panel b) shows the solar wind dynamic pressure during the flyby period. Panel c) shows a timeline of J-MAG sensor operation, with the lunar closest approach (LCA) and Earth closest approach (ECA) marked. Panel d) shows the distance of Juice from Earth.



the solar wind an auxiliary DC field of order 2000 nT is applied via the auxiliary coil solenoid fitted around the sensor optical axis. This lifts the field magnitude in the volume around the sensor way above the 100 nT limit, thus enabling detection of the external field component along the SCA optical axis with high accuracy. To compare fluxgate and SCA data in the solar wind, one must first project the measured vector from the fluxgates onto the SCA optical axis as it is only sensitive to the component
90 of the field strength along this direction.

The duration of the lunar pass was too short for SCA to heat up and stabilise, and with relatively low fields in the magnetotail, the auxiliary coil would be required. For these reasons it was agreed not to operate the SCA during the lunar pass. For the close approach to Earth, the challenge was to switch on while still in a low field environment with the auxiliary coil enabled and then switch off the auxiliary coil once the external field increased to a point where it was comfortably above the detection limit. The
95 approach taken for this was as follows.

SCA was switched on while still in a relatively low field environment, the cell and laser diode were heated to their operational temperatures, and the auxiliary coil was switched on to apply a constant DC field. Resonance sweeps were performed while operating in n_2 (longitudinal) resonance mode (Pollinger et al., 2012). This is the standard approach to get SCA into nominal field measurement mode. Then, as the external field increased, the auxiliary coil field was correspondingly ramped down such
100 that the field in the vicinity of the SCA sensor remained above 100 nT at all times in order to avoid losing lock. The timing of the auxiliary coil ramp down profile was estimated in advance by field modelling. As the angle between the external field and the optical axis strayed out of the n_2 operation cone, the SCA was switched to n_3 (transverse mode) at the start of the auxiliary coil ramp down. This was performed successfully, marking the first time in the mission that the n_3 mode was used. When the auxiliary coil current decreased to zero, SCA was free running in n_3 mode and measuring the true external field magnitude.
105 This is the first time the SCA was operated nominally, meaning that the angle of the magnetic field was taken from a fluxgate sensor, and based on this the resonance was chosen. This covered approximately four hours centred on the closest approach. There were two mode switches during the LEGA, from n_2 to n_3 and then back again. They happen at around 60° magnetic field angle, $0-60^\circ$ n_2 , and $60-90^\circ$ n_3 .

At external fields below 100 nT, a firm Zeeman resonance lock is not possible under all operating conditions. Here, generating
110 valid science data within the SCA specifications is also not possible (Ellmeier et al., 2024). As a consequence, SCA was switched back on with a constant auxiliary coil field some time later. SCA remained in that state from that point until the end of the J-MAG operational period. The timeline of SCA operation was executed as expected from the modelling predictions.

3 J-MAG measurements

In this section we examine J-MAG observations during the LEGA, broken down by region of interest. To assess performance,
115 we compare with other spacecraft measurements and empirical models when possible.



3.1 Earth flyby

We start by examining the performance of each of the sensors within Earth's magnetic field. Figure 3a shows the magnetic field magnitude measured by each of the three sensors in the two hours around closest approach. Artificial offsets of +100 nT and +200 nT have been added to IBS and OBS, respectively, in order to make all three traces visible. At this scale, the three measurements lie exactly on top of each other when plotted without offsets applied. Panel b) shows a zoom on the few minutes around peak field, but with no artificial offsets. OBS and IBS data are shown at a cadence of 16 Hz, while SCA is 1 Hz.

We can see that all signals are very clean, follow the expected pattern at close approach, and at the peak in field magnitude, the fluxgate sensors agree within 3 nT (out of ~ 4100 nT) of the scalar sensor. It is important to note that the data shown here have not yet undergone the final calibration process. Scaling and offsets determined during ground-based instrument testing have been applied, as well as preliminary in-flight offsets corrections determined in the solar wind using the well-established method of Hedgecock (1975). This is based, however, on relatively scarce data close to the LEGA period, and will be refined in future. It is also known that fluxgate magnetometer offsets are affected by changes in temperature. In the hours before closest approach, the J-MAG sensor temperatures varied significantly and did not have time to reach equilibrium before closest approach. No temperature-dependent adjustment has been applied at this early stage, however we already see excellent agreement between the sensors, which will only improve as calibration activities continue. Due to the temperature variations seen at OBS during the LEGA period, particularly due to the OBS heater which was required to be on during the inner cruise in order to load the power supply for SCA operation, IBS data were determined to be more reliable. The consolidated J-MAG data product used in this LEGA study is therefore constructed from IBS data. These are the data presented in the rest of this paper unless otherwise specified.

Figure 4 shows the magnetic field vector measured by J-MAG during the Earth flyby in GSE coordinates (thin, solid lines). Overlaid (thick, transparent lines) are the results of modelling the geomagnetic field expected to be seen over the flyby trajectory. The internal component of the field model comes from the latest version of the International Geomagnetic Reference Field model (IGRF-14; see Alken et al., 2021; Madsen et al., 2026). Externally-driven perturbations arising from solar wind interaction with the magnetosphere are then added using the Tsyganenko 2001 empirical model (see Tsyganenko, 2002a, b, for details), parametrised using solar wind measurements from OMNI during the flyby (i.e., those in Figure 2).

By comparing J-MAG observations with the modelled field, we can make an initial calibration estimate. Specifically, we look to see if there is any potential misalignment of the sensors with respect to the defined science coordinate systems. Initially, we see a maximum difference between the observations and model of around 40 nT. By performing a minimisation, we determined that a small rotation of less than 1° in each axis can reduce the maximum difference between the measured and modelled field at any point to ~ 20 nT, which we consider very good agreement in this high field environment. It is believed that much of the remaining discrepancy may be physical, instances where the models do not accurately capture the changing conditions, particularly on the edges of the flyby period. This aspect of calibration is ongoing and will be refined in future Earth flybys.

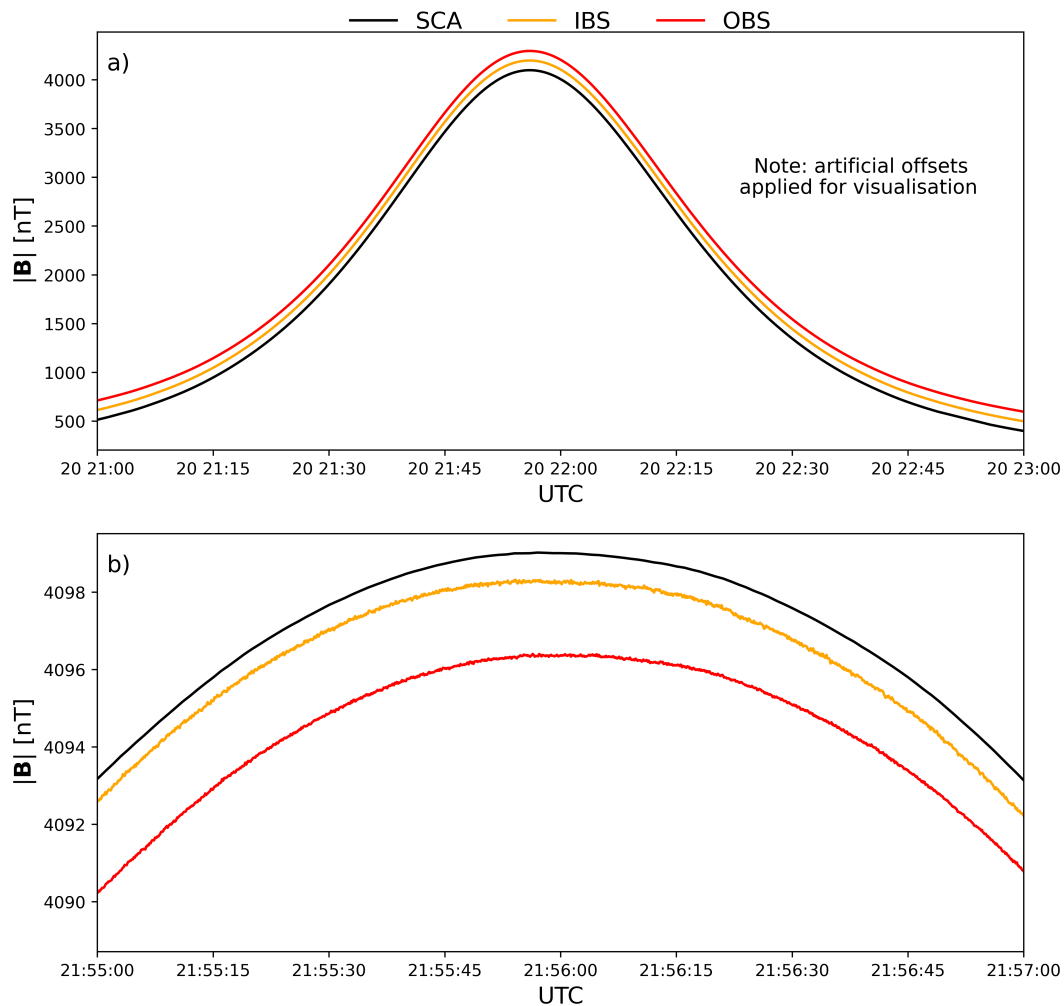


Figure 3. Magnetic field magnitude of the three J-MAG sensors around the Earth closest approach. Panel a) shows two hours centred on closest approach, with artificial offsets of +100 and +200 nT added to IBS and OBS data, respectively, to aid visualisation at this scale. Panel b) is a zoom on the peak field at the two minutes of closest approach (with no artificial offsets applied) showing slight differences between sensors. Note that this is not the final stage of calibration.

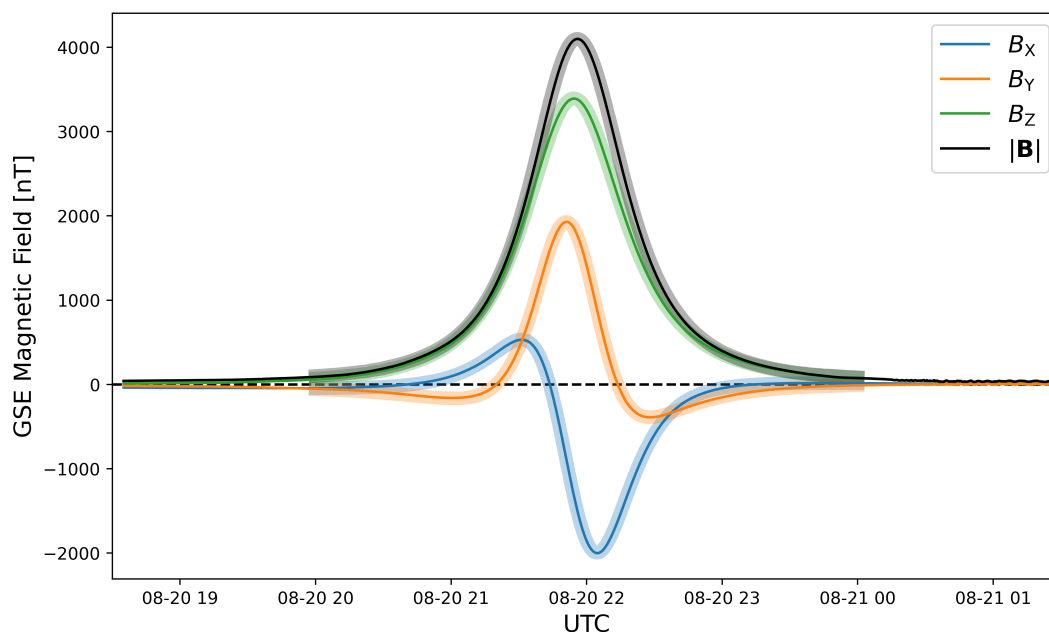


Figure 4. Magnetic field vector measured by J-MAG around Earth closest approach (solid lines), overlaid with model field from IGRF-14 and Tsyganenko 2001 model for the Juice LEGA trajectory (thick, transparent lines), all in GSE coordinate system.

3.2 Lunar flyby

Figure 5 shows the position (in GSE coordinates) of Juice relative to the Moon during the lunar phase of the LEGA. Also shown are the positions of the two spacecraft of the Acceleration, Reconnection, Turbulence and Electrodynamics of the Moon's Interaction with the Sun mission (ARTEMIS; Angelopoulos, 2011). These two probes were formerly part of the Time History of Events and Macroscale Interactions during Substorms mission (THEMIS; Angelopoulos, 2008), launched in 2007 in Earth orbit to study the dynamics of Earth's magnetosphere. In 2010, two of the five THEMIS probes were re-directed to enter a lunar orbit, where they continue to explore the magnetotail when the Moon is on the night side, and function as near-Earth solar wind monitors when the Moon is on the dayside. In Figure 5, Juice's position is shown in red, with ARTEMIS P1 and P2 in blue and purple, respectively, while the Moon is shown in grey. The lines show the trajectories over the period for which J-MAG was measuring, with the final positions of the bodies in this time period shown with markers.

Juice passed close to both the ARTEMIS probes, though significantly closer to P2. At the time of lunar closest approach (21:15), Juice was approximately 6,600 km ($\sim 1 R_E$) from ARTEMIS P2, and 16,600 km ($\sim 2.6 R_E$) from P1, while the two ARTEMIS probes were separated by 12,000 km ($\sim 1.9 R_E$). At these distances, one can expect very good agreement in the large-scale structures seen by all spacecraft, and we therefore find it interesting to compare J-MAG observations with those from the fluxgate magnetometers aboard ARTEMIS (Auster et al., 2008). This is shown in Figure 6 where the magnetic field measurements from all three spacecraft are shown in GSE. Data for all three spacecraft are shown at 16 Hz. Here we show

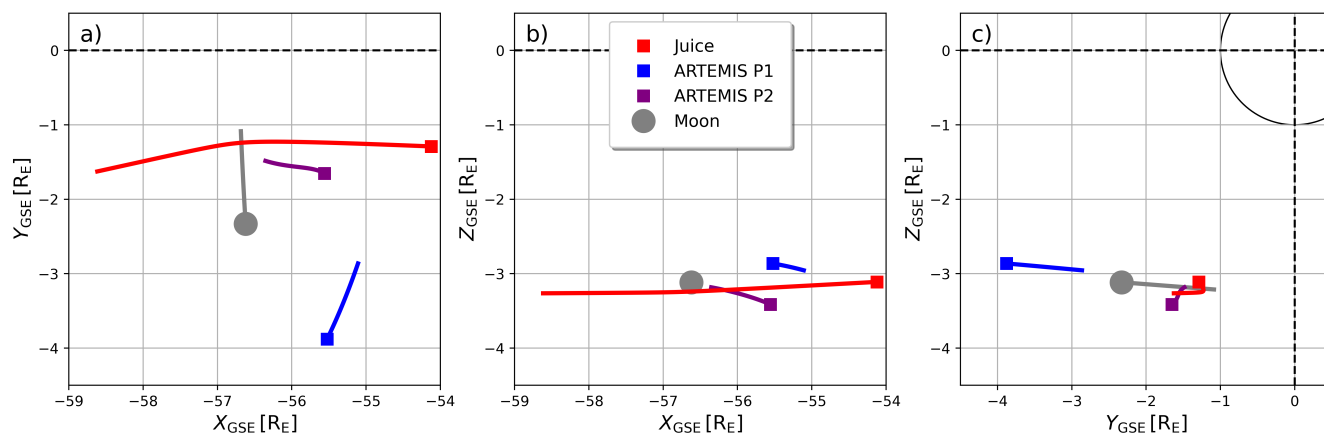


Figure 5. Orbital trajectories of Juice, the two ARTEMIS probes, and the Moon during the lunar pass, 19 Aug 20:20–22:30. All positions in Earth radii, GSE coordinate system, shown in all three planes. Final positions of the bodies in this period indicated with markers.

OBS and IBS data separately, with OBS in red and IBS in yellow. Offsets of the J-MAG sensors have been adjusted to best match ARTEMIS data for this comparison. The shaded area marks the time for which Juice was in eclipse, and a vertical line marks the point of closest approach to the Moon.

We can make several observations from this short window of data. It is immediately noticeable that both J-MAG sensors show very clean signals, with the level of noise significantly lower than in the corresponding ARTEMIS measurements. This is yet another excellent demonstration of the instrument quality and magnetic cleanliness of the spacecraft (Engelke et al., 2023). Over the two-hour period, the field is dominated by a strong X-component, which makes sense given the position in the magnetotail. Overall, the observed fields are relatively stable, with the maximum field variation around 2 nT. This makes for an excellent opportunity to probe any differences in the four signatures.

There are some discrepancies between the two ARTEMIS probes. This is most notable in the GSE Z axis, where they report a difference of up to about 1 nT in the latter portion of the flyby. While curious, this is not totally unexpected given their spatial separation. More puzzling, however, are the differences seen between the two J-MAG sensors. The second half of the flyby, after closest approach, shows generally good agreement, however, significant differences are seen in the earlier portion of the flyby. We see that OBS measures a larger field magnitude, primarily in the GSE X axis, and is at points nearly 1 nT larger than IBS and around 0.6 nT larger than the two ARTEMIS probes. In this period IBS generally sits at a lower magnitude than ARTEMIS, and shows an amount of fluctuation.

We offer some possible explanations for these discrepancies. The lunar pass occurred almost immediately after the instrument was switched on. This means that there was a steep temperature gradient at the time as the sensors and electronics began to warm up. The period of eclipse is also likely to have had an effect on the instrument temperatures, both in terms of the shadow, and the restricted operation of other spacecraft processes while running from battery power. As discussed earlier, temperature is known to affect magnetometer offsets, which may explain the differing behaviour of IBS and OBS. It appears that

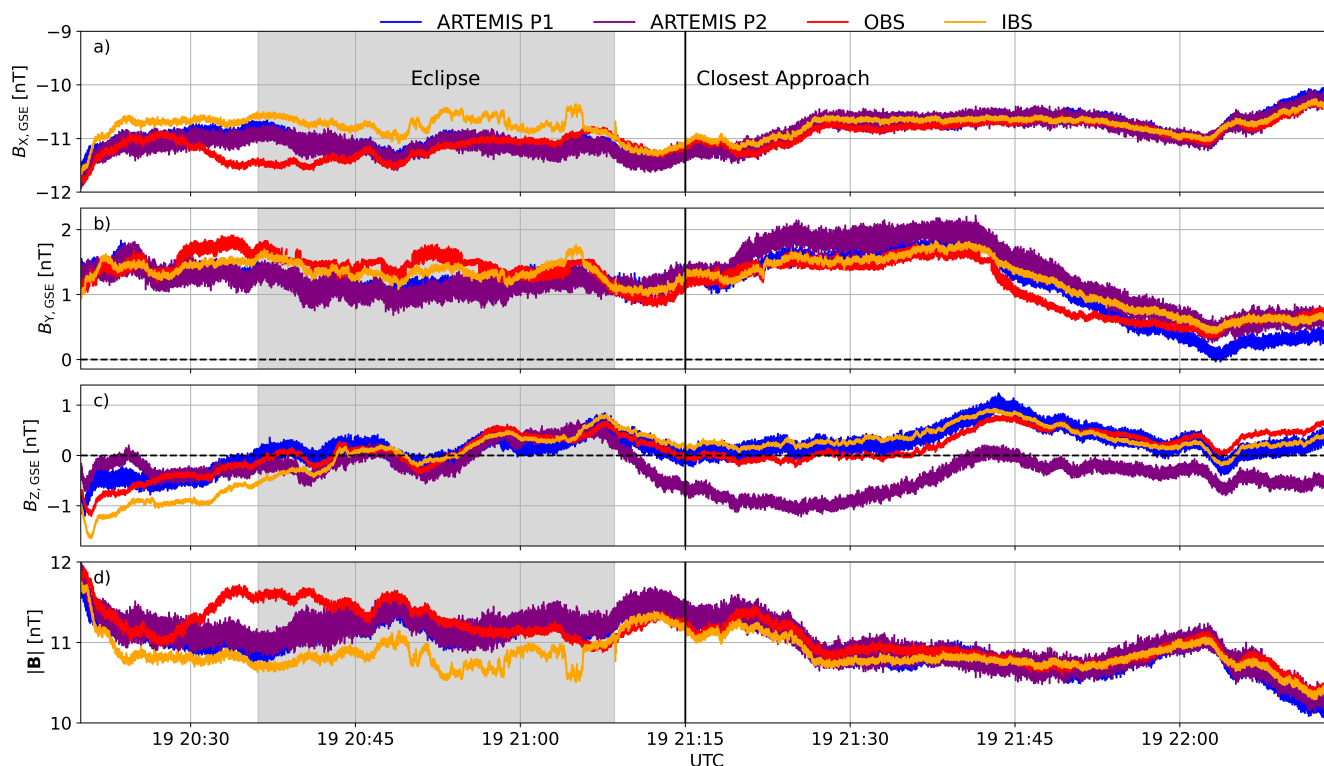


Figure 6. Magnetic field measurements from J-MAG OBS and IBS during the lunar pass, overlaid with observations from the two ARTEMIS probes, all in the GSE coordinate system. Panel d) shows the field magnitudes. Shaded area indicates the period in which the spacecraft was in an eclipse, and the solid vertical line marks the time of lunar closest approach.

185 these irregularities mostly settled after around an hour of operation. In future we would recommend that J-MAG be switched on several hours in advance of any period considered crucial for recording science or calibration data in order to allow for temperature equilibrium to be reached.

As well as relative drifts between the two J-MAG sensors, there were also some sharp disturbances of order ~ 0.5 nT seen by IBS during the eclipse period, most notably at around 21:05, and primarily in the GSE X and Y axes. These axes were determined to be roughly perpendicular to the axis of the magnetometer boom during this period. It is therefore believed that a current source along the boom harness may be responsible for the signal seen by IBS, which would also explain why it was not seen by OBS, which is mounted further along the boom. This is a subject of ongoing investigation, in collaboration with other Juice instrument teams. Despite the initial calibration, unstable temperatures, and possible electrical disturbances, we consider the overall performance of J-MAG during the lunar phase to be very encouraging. It has provided several areas of investigation and calibration activities, and helps planning of future flyby operations.

190
195

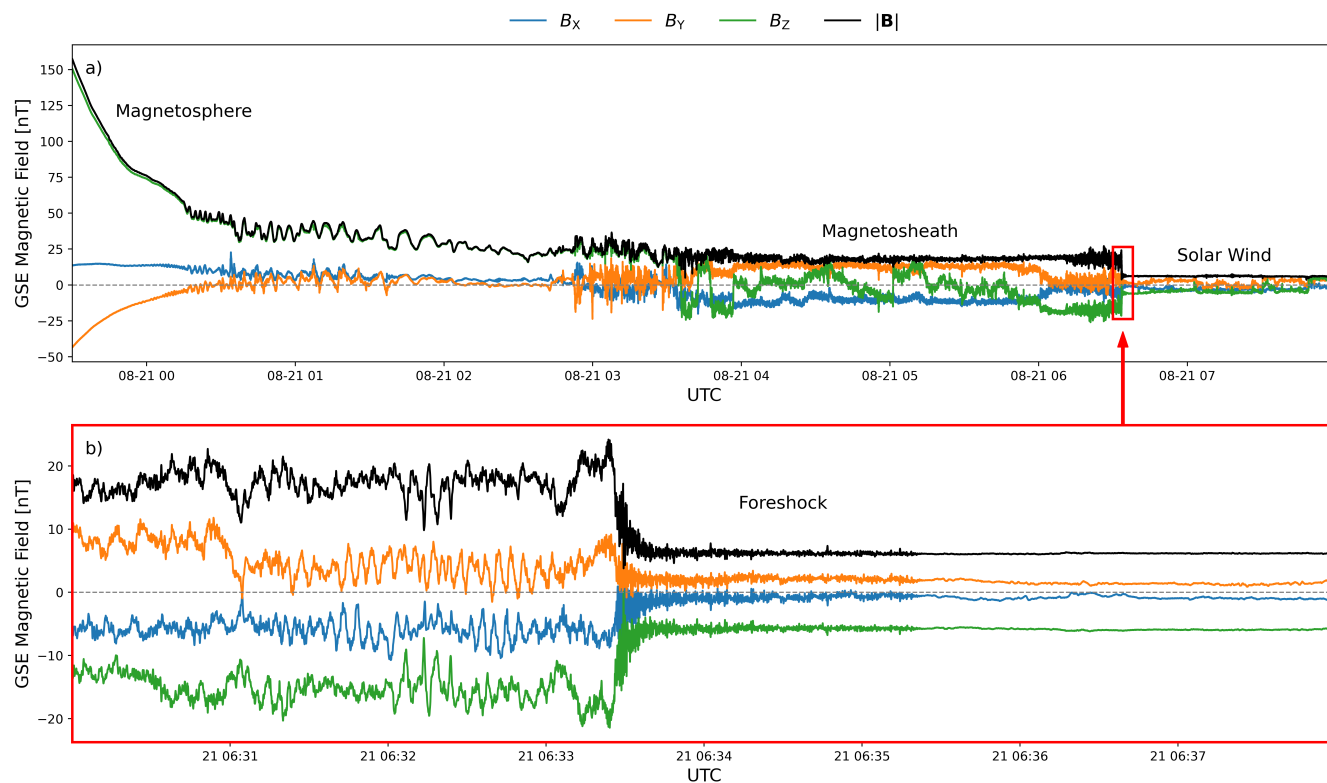


Figure 7. J-MAG magnetic field measurements (GSE) during magnetospheric exit on 21 August. Panel a) shows the field vector and magnitude as the spacecraft transited the magnetosheath and entered the solar wind. Panel b) shows a zoom of the bow shock crossing (red square in top panel).

3.3 Outer magnetosphere and solar wind

The longest portion of continuous operation during the LEGA occurred after the spacecraft exited the magnetosphere. In this section we take a closer look at its transit through the magnetosheath and entry into the solar wind. Figure 7a shows J-MAG measurements in GSE across an 8-hour period covering the magnetospheric exit, from the outer magnetosphere on the left, through the magnetopause and magnetosheath, across the bow shock, and into the solar wind. Figure 7b is a zoom of the red box drawn on the upper panel, which shows the shock crossing in detail over a period of 8 minutes.

Before leaving the magnetosphere, J-MAG saw significant field oscillations from around 00:15 until 02:30. These oscillations take place in a background field of around 40 nT (though gradually decreasing throughout), with amplitudes of order 10 nT and periods between 1 and 9 minutes, increasing with proximity to the magnetopause. Given these scales, it seems likely that these are MHD-scale ultra low frequency (ULF) oscillations (Pc5 band), perhaps associated with field line resonances (e.g., Chen and Hasegawa, 1974), global cavity modes (e.g., Kivelson and Southwood, 1985), or Kelvin Helmholtz instabilities (e.g., Southwood, 1968). The magnetopause crossing itself is poorly defined, with several possible partial crossings in quick



210 succession (seen by field rotations, predominantly B_Z , at the current sheet boundary), and a possible pile up layer. After this, Juice entered the magnetosheath. That is, a region of shocked, slowed, compressed solar wind. The field magnitude in this period is around 18 nT, though a degree of high-frequency fluctuations and occasional field rotations are seen. This is consistent with known properties of the turbulent magnetosheath (e.g., Zhang et al., 2019).

215 The bow shock crossing shown in Figure 7b is much more abrupt than the magnetopause crossing, and shows the expected structure of a quasi-perpendicular shock with a foot, ramp, and overshoot (e.g., Bale et al., 2005). The shock-normal to interplanetary magnetic field angle is around 70° , calculated using the magnetic coplanarity theorem. Upstream of the shock, there is a short foreshock with high-frequency fluctuations, perhaps kinetic whistler waves (e.g., Zhang et al., 1998), lasting approximately 2 minutes for Juice's passage (from 06:33:30 to 06:35:20). This corresponds to around 440 km in space. Downstream of the shock (left side of plot) we see some evidence for mirror mode waves, which often can be seen in high β plasma downstream of perpendicular shocks and exhibit proportionally large fluctuations in $|\mathbf{B}|$, though further investigation (including plasma moments) would be needed to confirm this.

220 While there is clearly a wealth of physical interest in this short interval, we do not explore it further in this paper, but note once again that this is an excellent demonstration of J-MAG's ability to observe such phenomena, which is very promising for future endeavours at Jupiter and Ganymede, where we expect to see similar field magnitudes to some of the outer magnetospheric regions explored here.

225 Figure 8 shows J-MAG measurements (red) at a 1-minute cadence over several days, after Juice exited the magnetosphere and was travelling duskward through the solar wind. Overlaid are corresponding measurements from the OMNI database (grey), sampled at L1 and propagated to Earth's bow shock, also at 1-minute cadence. Note that this is the same data shown in the latter half of Figure 2a. No timing adjustments have been made to either dataset, though given Juice remained marginally sunward of the terminator in this period, we would perhaps expect the solar wind observations to be similar to those seen at Earth.

230 On large scales, the two datasets agree remarkably well, both in terms of absolute magnitudes and in vector fluctuations. This is another excellent validation of J-MAG's performance. We do see some notable differences on smaller scales, however, particularly towards the second half of the dataset, where there are several instances of rotational discontinuities seen by Juice but not captured by OMNI, and we notice that the temporal alignment of observed structures also worsens. This is largely expected, as while Juice is relatively close (around $30 R_E$) to the Sun-Earth line at the start of this interval, by the end it was around $150 R_E$. It is well-known that spatial structures in the solar wind can vary considerably on this scale (e.g., Borovsky, 2018).

240 Despite these differences, there is a generally very good correspondence between the two datasets. This also demonstrates the potential utility of Juice (and other planetary missions) during cruise phase as solar wind monitors for the purposes of space weather forecasting and post-event analysis, if the science payload is active and the data can be transmitted to ground with low latency. The often unusual orbits of these missions during cruise can allow for sampling of regions of the heliosphere not regularly covered. In terms of space weather, this can become particularly useful if the spacecraft maintain good alignment with the Sun-Earth line or move sunward of L1. This has been successfully trialled with Solar Orbiter (see, e.g., Laker et al.,

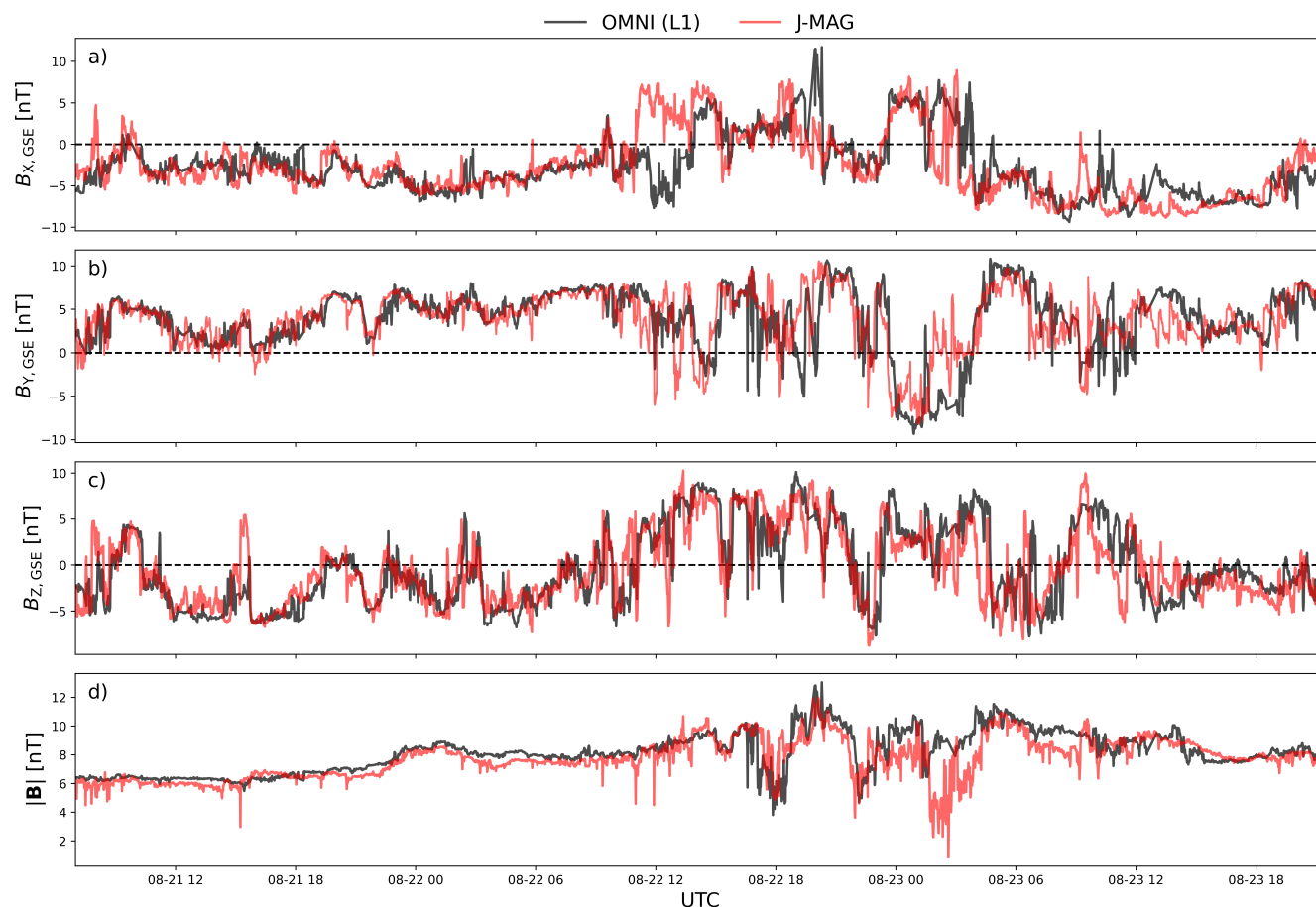


Figure 8. Comparison of J-MAG measurements (red) with those from OMNI (measured at L1, grey), over several days in the solar wind after the LEGA. During this time, Juice moved around $120 R_E$ duskward from Earth. All field vectors shown in GSE coordinate system.

2024, for predictions of CME arrival times using magnetometer data from Solar Orbiter), and we would argue that planetary missions should be used to the same end when in cruise, though this would require the science payload to be operational more often than is typical.

4 Summary and conclusions

In this paper, we have presented the first results from the Juice magnetometer during the Lunar-Earth gravity assist of August 2024. We have demonstrated the excellent performance of all three J-MAG sensors during this period, despite in-flight calibration being only preliminary at this stage in the mission. The operation of the scalar sensor in this environment proved challenging but was executed successfully. The flyby's interesting trajectory allowed for several opportunities to validate J-MAG



observations against those from other spacecraft and models. During the lunar pass we compared J-MAG with ARTEMIS, seeing good agreement in the latter half of the short window. At the close approach to Earth, we used the IGRF-14 and Tsyganenko 2001 models to calculate an approximate value for sensor misalignment, finding it to be less than 1° , and seeing very good agreement with the predicted geomagnetic field. In the solar wind, we were able to compare J-MAG data with those measured at L1 (from OMNI), also finding excellent agreement despite increasingly large spatial separation. This showed the potential utility of using Juice as a solar wind monitor during the cruise phase, if the science payload is operational. We also highlighted several regions of interest for further study during magnetospheric exit, with the preliminary results proving promising for the Ganymede phase of the mission.

We have learned of several areas for future calibration activities and made suggestions for future operations. In order to improve calibration, stable temperatures are required, suggesting J-MAG should be switched on well in advance of encountering any body of interest. Temperature-dependent scaling can also be made when more flight data are available to study the effects. With more time operating in the solar wind, we can build up a better understanding of in-flight offset adjustments, and the two upcoming Earth flybys present further opportunities for alignment calibration. Part of this will also include operating the Juice Magnetometer Alignment Calibration System (JACS), the study of which during the LEGA is ongoing. Future EGAs will also include opportunities to calibrate the fluxgate sensors against data from the scalar sensor.

Overall, J-MAG performance during the LEGA was excellent, and we look forward to the next Earth gravity assist in September 2026.

Data availability. The J-MAG data from the LEGA are currently under the mission's cruise-phase proprietary period and will be released publicly in the first Cruise Archive Delivery in 2029. OMNI data can be accessed through NASA/GSFC's OMNIWeb: https://omniweb.gsfc.nasa.gov/ow_min.html. THEMIS/ARTEMIS data are available from the mission archive: <https://themis.ssl.berkeley.edu/data/themis/>.

Author contributions. ATL prepared the manuscript with assistance from PB and LS. Data preparation and analysis was performed by ATL, LS, AB, DH, PB, HC, XY, TP, AS, and VG. Instrumentation development and LEGA execution performed by MKD, PB, H-UA, WM, IJ, CA, RB, AS, LS, RL, FP, AM, and DH. All authors reviewed and edited the manuscript.

Competing interests. The authors declare that they have no conflict of interest.

Acknowledgements. The Imperial College London LEGA operations team were supported by the UK Space Agency award ST/X002357/1. The work by LS, HUA, and FP was financially supported by the German Center for Aviation and Space (DLR) under contract 50 QJ 2402. The work at IWF Graz was supported by funding contributions from the Austrian Space Applications Program of the Austrian Research Promotion Agency (grant number FO999911907). We acknowledge use of NASA/GSFC's Space Physics Data Facility's OMNIWeb service, and OMNI

<https://doi.org/10.5194/egusphere-2026-2054>

Preprint. Discussion started: 15 April 2026

© Author(s) 2026. CC BY 4.0 License.



280 data. We acknowledge NASA contract NAS5-02099 and V. Angelopoulos for use of data from the THEMIS Mission. Specifically: K. H. Glassmeier, U. Auster and W. Baumjohann for the use of FGM data provided under the lead of the Technical University of Braunschweig and with financial support through the German Ministry for Economy and Technology and the German Center for Aviation and Space (DLR) under contract 50 OC 0302.



References

- Alken, P., Thébault, E., Beggan, C. D., Amit, H., Aubert, J., Baerenzung, J., Bondar, T. N., Brown, W. J., Califf, S., Chambodut, A., Chulliat, A., Cox, G. A., Finlay, C. C., Fournier, A., Gillet, N., Grayver, A., Hammer, M. D., Holschneider, M., Huder, L., Hulot, G., Jager, T., Kloss, C., Korte, M., Kuang, W., Kuvshinov, A., Langlais, B., Léger, J.-M., Lesur, V., Livermore, P. W., Lowes, F. J., Macmillan, S., Magnes, W., Manda, M., Marsal, S., Matzka, J., Metman, M. C., Minami, T., Morschhauser, A., Mound, J. E., Nair, M., Nakano, S., Olsen, N., Pavón-Carrasco, F. J., Petrov, V. G., Ropp, G., Rother, M., Sabaka, T. J., Sanchez, S., Saturnino, D., Schnepf, N. R., Shen, X., Stolle, C., Tangborn, A., Tøffner-Clausen, L., Toh, H., Torta, J. M., Varner, J., Vervelidou, F., Vigneron, P., Wardinski, I., Wicht, J., Woods, A., Yang, Y., Zeren, Z., and Zhou, B.: International Geomagnetic Reference Field: the thirteenth generation, *Earth, Planets and Space*, 73, 49, <https://doi.org/10.1186/s40623-020-01288-x>, 2021.
- Amtmann, C., Pollinger, A., Ellmeier, M., Dougherty, M., Brown, P., Lammegger, R., Betzler, A., Agú, M., Hagen, C., Jernej, I., Wilfinger, J., Baughen, R., Strickland, A., and Magnes, W.: Accuracy of the scalar magnetometer aboard ESA's JUICE mission, *Geoscientific Instrumentation, Methods and Data Systems*, 13, 177–191, <https://doi.org/10.5194/gi-13-177-2024>, 2024.
- Angelopoulos, V.: The THEMIS mission, *Space Science Reviews*, 141, 5–34, <https://doi.org/10.1007/s11214-008-9336-1>, 2008.
- Angelopoulos, V.: The ARTEMIS Mission, *Space Science Reviews*, 165, 3–25, <https://doi.org/10.1007/s11214-010-9687-2>, 2011.
- Auster, H. U., Apathy, I., Berghofer, G., Remizov, A., Roll, R., Fornaçon, K. H., Glassmeier, K. H., Haerendel, G., Hejja, I., Kührt, E., Magnes, W., Moehlmann, D., Motschmann, U., Richter, I., Rosenbauer, H., Russell, C. T., Rustenbach, J., Sauer, K., Schwingschuh, K., Szemerey, I., and Waesch, R.: ROMAP: Rosetta Magnetometer and Plasma Monitor, *Space Science Reviews*, 128, 221–240, <https://doi.org/10.1007/s11214-006-9033-x>, 2007.
- Auster, H. U., Glassmeier, K. H., Magnes, W., Aydogar, O., Baumjohann, W., Constantinescu, D., Fischer, D., Fornaçon, K. H., Georgescu, E., Harvey, P., Hillenmaier, O., Kroth, R., Ludlam, M., Narita, Y., Nakamura, R., Okrafka, K., Plaschke, F., Richter, I., Schwarzl, H., Stoll, B., Valavanoglou, A., and Wiedemann, M.: The THEMIS Fluxgate Magnetometer, *Space Science Reviews*, 141, 235–264, <https://doi.org/10.1007/s11214-008-9365-9>, 2008.
- Bale, S. D., Balikhin, M. A., Horbury, T. S., Krasnoselskikh, V. V., Kucharek, H., Möbius, E., Walker, S. N., Balogh, A., Burgess, D., Lembège, B., Lucek, E. A., Scholer, M., Schwartz, S. J., and Thomsen, M. F.: Quasi-perpendicular Shock Structure and Processes, *Space Science Reviews*, 118, 161–203, <https://doi.org/10.1007/s11214-005-3827-0>, 2005.
- Borovsky, J. E.: The Spatial Structure of the Oncoming Solar Wind at Earth and the Shortcomings of a Solar-Wind Monitor at L1, *Journal of Atmospheric and Solar-Terrestrial Physics*, 177, 2–11, <https://doi.org/10.1016/j.jastp.2017.03.014>, 2018.
- Chen, L. and Hasegawa, A.: A theory of long-period magnetic pulsations: 1. Steady state excitation of field line resonance, *Journal of Geophysical Research (1896-1977)*, 79, 1024–1032, <https://doi.org/10.1029/JA079i007p01024>, 1974.
- Dougherty, M. K., Kellock, S., Southwood, D. J., Balogh, A., Smith, E. J., Tsurutani, B. T., Gerlach, B., Glassmeier, K.-H., Gleim, F., Russell, C. T., Erdos, G., Neubauer, F. M., and Cowley, S. W. H.: The Cassini Magnetic Field Investigation, *Space Science Reviews*, 114, 331–383, <https://doi.org/10.1007/s11214-004-1432-2>, 2004.
- Ellmeier, M., Betzler, A., Amtmann, C., Pollinger, A., Hagen, C., Jernej, I., Agú, M., Magnes, W., Windholz, L., Dougherty, M., Brown, P., and Lammegger, R.: Lower magnetic field measurement limit of the coupled dark state magnetometer, *Measurement Science and Technology*, 35, 115 110, <https://doi.org/10.1088/1361-6501/ad6623>, 2024.



- Engelke, S., Bubeck, K., Baroni, M., Kiss, Z., Verstaen, S., Lange, J., and Faust, M.: Verification of the JUICE Spacecraft Magnetic Cleanliness and Emitted Field Modelling, in: 2023 Photonics Electromagnetics Research Symposium (PIERS), pp. 1250–1259, <https://doi.org/10.1109/PIERS59004.2023.10221546>, 2023.
- Grasset, O., Dougherty, M. K., Coustenis, A., Bunce, E. J., Erd, C., Titov, D., Blanc, M., Coates, A., Drossart, P., Fletcher, L. N., Hussmann, H., Jaumann, R., Krupp, N., Lebreton, J.-P., Prieto-Ballesteros, O., Tortora, P., Tosi, F., and Hoolst, T. V.: JUPITER ICy moons Explorer (JUICE): An ESA mission to orbit Ganymede and to characterise the Jupiter system, *Planetary and Space Science*, 78, 1–21, <https://doi.org/https://doi.org/10.1016/j.pss.2012.12.002>, 2013.
- Hedgecock, P. C.: A correlation technique for magnetometer zero level determination., *Space Science Instrumentation*, 1, 83–90, 1975.
- Heyner, D., Auster, H.-U., Fornaçon, K.-H., Carr, C., Richter, I., Mieth, J. Z. D., Kolhey, P., Exner, W., Motschmann, U., Baumjohann, W., Matsuoka, A., Magnes, W., Berghofer, G., Fischer, D., Plaschke, F., Nakamura, R., Narita, Y., Delva, M., Volwerk, M., Balogh, A., Dougherty, M., Horbury, T., Langlais, B., Manda, M., Masters, A., Oliveira, J. S., Sánchez-Cano, B., Slavin, J. A., Vennerstrøm, S., Vogt, J., Wicht, J., and Glassmeier, K.-H.: The BepiColombo Planetary Magnetometer MPO-MAG: What Can We Learn from the Hermean Magnetic Field?, *Space Science Reviews*, 217, 52, <https://doi.org/10.1007/s11214-021-00822-x>, 2021.
- Horbury, T. S., O'Brien, H., Blazquez, I. C., Bendyk, M., Brown, P., Hudson, R., Evans, V., Oddy, T. M., Carr, C. M., Beek, T. J., Cupido, E., Bhattacharya, S., Dominguez, J.-A., Matthews, L., Myklebust, V. R., Whiteside, B., Bale, S. D., Baumjohann, W., Burgess, D., Carbone, V., Cargill, P., Eastwood, J., Erdős, G., Fletcher, L., Forsyth, R., Giacalone, J., Glassmeier, K.-H., Goldstein, M. L., Hoeksema, T., Lockwood, M., Magnes, W., Maksimovic, M., Marsch, E., Matthaeus, W. H., Murphy, N., Nakariakov, V. M., Owen, C. J., Owens, M., Rodriguez-Pacheco, J., Richter, I., Riley, P., Russell, C. T., Schwartz, S., Vainio, R., Velli, M., Vennerstrom, S., Walsh, R., Wimmer-Schweingruber, R. F., Zank, G., Müller, D., Zouganelis, I., and Walsh, A. P.: The Solar Orbiter magnetometer, *Astronomy & Astrophysics*, 642, A9, <https://doi.org/10.1051/0004-6361/201937257>, 2020.
- King, J. H. and Papitashvili, N. E.: Solar wind spatial scales in and comparisons of hourly Wind and ACE plasma and magnetic field data, *Journal of Geophysical Research: Space Physics*, 110, 1–9, <https://doi.org/10.1029/2004JA010649>, 2005.
- Kivelson, M. G. and Southwood, D. J.: Resonant ULF waves: A new interpretation, *Geophysical Research Letters*, 12, 49–52, <https://doi.org/https://doi.org/10.1029/GL012i001p00049>, 1985.
- Laker, R., Horbury, T. S., O'Brien, H., Fauchon-Jones, E. J., Angelini, V., Fargette, N., Amerstorfer, T., Bauer, M., Möstl, C., Davies, E. E., Davies, J. A., Harrison, R., Barnes, D., and Dumbović, M.: Using Solar Orbiter as an Upstream Solar Wind Monitor for Real Time Space Weather Predictions, *Space Weather*, 22, e2023SW003628, <https://doi.org/https://doi.org/10.1029/2023SW003628>, e2023SW003628, 2024.
- Madsen, F. D., Beggan, C. D., Brown, W. J., Holme, R., Lauridsen, J. B., and Whaler, K. A.: IGRF-14 secular variation prediction from core surface flow acceleration, *Earth, Planets and Space*, 78, 29, <https://doi.org/10.1186/s40623-025-02347-x>, 2026.
- Pollinger, A., Ellmeier, M., Magnes, W., Hagen, C., Baumjohann, W., Leitgeb, E., and Lammegger, R.: Enable the inherent omnidirectionality of an absolute coupled dark state magnetometer for e.g. scientific space applications, in: 2012 IEEE International Instrumentation and Measurement Technology Conference Proceedings, pp. 33–36, <https://doi.org/10.1109/I2MTC.2012.6229247>, 2012.
- Pollinger, A., Lammegger, R., Magnes, W., Hagen, C., Ellmeier, M., Jernej, I., Leichtfried, M., Kürbisch, C., Maierhofer, R., Wallner, R., Fremuth, G., Amtmann, C., Betzler, A., Delva, M., Prattes, G., and Baumjohann, W.: Coupled dark state magnetometer for the China Seismo-Electromagnetic Satellite, *Measurement Science and Technology*, 29, 095 103, <https://doi.org/10.1088/1361-6501/aacde4>, 2018.



- 355 Shue, J.-H., Song, P., Russell, C. T., Steinberg, J. T., Chao, J. K., Zastenker, G., Vaisberg, O. L., Kokubun, S., Singer, H. J., Detman, T. R.,
and Kawano, H.: Magnetopause location under extreme solar wind conditions, *Journal of Geophysical Research: Space Physics*, 103,
17 691–17 700, <https://doi.org/10.1029/98ja01103>, 1998.
- Southwood, D.: The hydromagnetic stability of the magnetospheric boundary, *Planetary and Space Science*, 16, 587–605,
[https://doi.org/10.1016/0032-0633\(68\)90100-1](https://doi.org/10.1016/0032-0633(68)90100-1), 1968.
- Tsyganenko, N. A.: A model of the near magnetosphere with a dawn-dusk asymmetry 1. Mathematical structure, *Journal of Geophysical*
360 *Research: Space Physics*, 107, SMP 12–1–SMP 12–15, <https://doi.org/10.1029/2001JA000219>, 2002a.
- Tsyganenko, N. A.: A model of the near magnetosphere with a dawn-dusk asymmetry 2. Parameterization and fitting to observations, *Journal*
of Geophysical Research: Space Physics, 107, SMP 10–1–SMP 10–17, <https://doi.org/10.1029/2001JA000220>, 2002b.
- Zhang, H., Fu, S., Pu, Z., Lu, J., Zhong, J., Zhu, C., Wan, W., and Liu, L.: Statistics on the Magnetosheath Properties Related to Magnetopause
Magnetic Reconnection, *The Astrophysical Journal*, 880, 122, <https://doi.org/10.3847/1538-4357/ab290e>, 2019.
- 365 Zhang, Y., Matsumoto, H., and Kojima, H.: Bursts of whistler mode waves in the upstream of the bow shock: Geotail observations, *Journal*
of Geophysical Research: Space Physics, 103, 20 529–20 540, <https://doi.org/10.1029/98JA01371>, 1998.